Report Written By: Kamazima Lwiza & Gordon Taylor **Date:** 08/22/2012

A. Project Number and Title: R/CMB-35-NYCT "***Interaction of biological and physical factors controlling bottom dissolved oxygen***."

B. Project Personnel:

Elizabeth Suter
Ling Liu
Gordon Taylor
Kamazima Lwiza

C. Project Results:

C1. Meeting the Objectives:

Objective 1: Identify mechanisms (anthropogenic and natural) that influence the interannual variability in dissolved nutrients, winter temperature, light availability, phytoplankton biomass, and dissolved oxygen.

This part of our study was designed to identify the effectiveness of TMDLs on water quality in LIS over a 15 year period (January 1995 to May 2009) by identifying changes in nutrient stoichiometry, temperature, light availability, phytoplankton community structure, and dissolved oxygen patterns that have occurred since the 1990s, when the TMDLs were first implemented.

Data & Methods:

Nutrients, chlorophyll *a*, and hydrographic data were obtained from the Connecticut Department of Energy and Environmental Protection's (CTDEEP) database (available at http://lisicos.uconn.edu/). For this analysis, data from 2 depths (surface and bottom) at 9 stations along Long Island Sound's primary axis were tabulated between January 1995 and May 2009. The stations included A4, B3, C2, D3, E1, H4, I2, J2, and M3 (Fig. 1.1). Each survey included continuous depth profiles of density, temperature, salinity, and dissolved oxygen. Discrete Niskin bottle samples were analyzed for concentrations of particulate biogenic silica (BioSi), chlorophyll a (Chl*a*), orthophosphate (DIP), dissolved organic carbon (DOC), ammonium (NH_4^+), nitrate + nitrite (NO_x), particulate carbon (PC), particulate nitrogen (PN), particulate phosphorus (PP), dissolved silica (DSi), total dissolved nitrogen (TDN), total dissolved phosphorus (TDP), and total suspended solids (TSS). Collection and analytical methods used by CTDEEP are available on the website (http://lisicos.uconn.edu/). To avoid infinite DIN:DIP ratios we used an excess DIN index (DINxs) calculated as (Hansell et al., 2004):

$$DINxs = DIN - 16 \times DIP$$

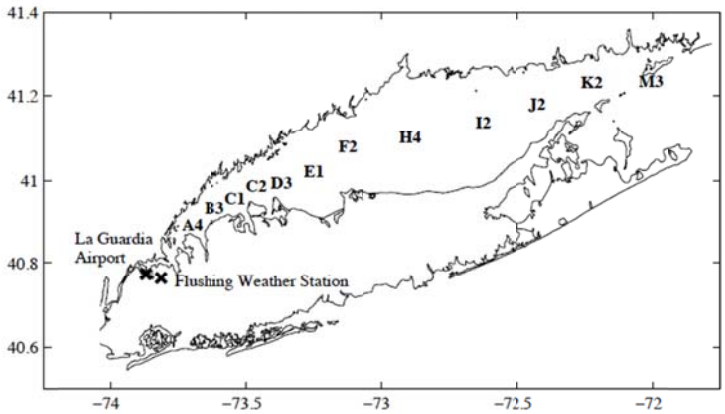

Figure 1.1: Map of Long Island Sound showing CTDEEP sampling stations

The CTDEEP also provides data on phytoplankton community composition obtained by pigment analysis starting from April 2002. Pigment concentrations are measured using High Performance Liquid Chromatography (HPLC), compared to known photopigment ratios of communities from LIS, and analyzed on Chemtax in order to estimate the contribution by each group (CTDEEP, 2005). All samples were taken from a depth of 2m. Analyzed taxonomical groups of phytoplankton included *Bacillariophyceae* (diatoms), *Dinophyceae* (dinoflagellates), cyanobacteria, *Prasinophyceae*, *Chlorophyceae*, *Cryptophyceae*, *Prymnesiophyceae* A & B, *Raphidophyceae*, *Eustigmatophyceae*, *Chrysophyceae*, and *Euglenophyceae*.

Meteorological data were also compared with nutrients and phytoplankton data. Monthly precipitation totals from La Guardia Airport were downloaded from NOAA (http://lwf.ncdc.noaa.gov/oa/ncdc.html). Cloud cover (reported as percent cloud cover) and wind speed at the Flushing weather station were obtained from Weather Underground (http://www.wunderground.com). Wind speed was converted to wind energy by squaring the speed. The Connecticut River contributes >70% of the riverine freshwater being discharged into Long Island Sound, and thus it is a good representation of the estimate of freshwater input (Lee and Lwiza 2005). Monthly freshwater discharge from the Connecticut River was downloaded from USGS (http://waterdata.usgs.gov/nwis).

Long-term trends of nutrients, Chl*a*, and the phytoplankton clades were calculated using the Theil-Sen (T-S) estimator, a robust regression method which takes into account the possibility the data being heteroscedastic (Wilcox, 2005). Confidence intervals (CI) were estimated by bootstrapping 599 estimates of either the T-S estimator and taking the middle 95% of these estimates, according to Wilcox (2005). Canonical component analysis (CCA) was used for multivariate analysis according to the Barnett and Preisendorfer (1987) method. Nutrient, hydrographic, and phytoplankton variables at station A4 were split into 3 datasets, pre-filtered using principal component analysis, and CCA was used to determine the patterns of maximum correlation between the 3 datasets. After pre-filtering, this method was used to determine the patterns for different modes that maximize the covariance between phytoplankton and nutrient variables or between phytoplankton and hydrographic variables.

Results:
Dissolved nitrogen species changed significantly between 1995 and 2009 at all stations in LIS. TDN concentrations, which include DIN and DON, have increased in both surface and bottom waters (Fig. 1.2A), with the largest increases being in western LIS. DON concentrations have significantly increased at all stations in surface and bottom waters (Fig. 1.2B). In contrast, DIN concentrations decreased significantly at most stations, except A4, where they increased (Fig. 1.2C). The modest decreases in DIN concentrations at most stations were largely driven by decreases in concentrations of NO_x (Fig. 1.2D). There were no consistent trends in NH_4^+ concentrations, except at A4, where they significantly increased in surface and bottom waters (Fig. 1.2 E). In general, the inorganic dissolved nitrogen species have decreased Sound-wide in favor of increases in dissolved organic forms. Station A4 is an exception, where both the inorganic and organic dissolved nitrogen species increased.

TDP concentrations have significantly increased throughout the Sound in surface and bottom waters (Fig. 1.3A). The largest increases were observed in western LIS. No measureable changes in DOP concentrations were observed at any station. At the same time DIP concentrations show a significant increase in surface and bottom waters for all stations, with the largest changes also observed in western LIS (Fig. 1.3B).

DSi concentrations increased significantly throughout the Sound in surface and bottom waters (Fig. 1.4A). However, particulate BioSi significantly decreased at all stations in surface and bottom waters (Fig. 1.4B). Western LIS exhibited the largest changes. Increases in DSi were generally larger than decreases in BioSi, and so total Si significantly increased at most stations.

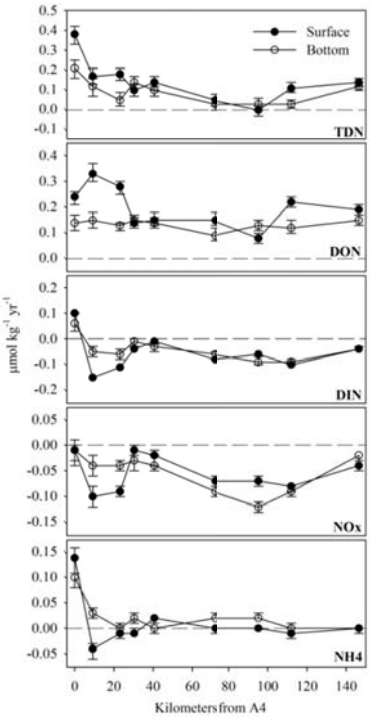

Figure 1.2: Rates of change in concentrations of (A) total dissolved nitrogen (TDN), (B) dissolved organic nitrogen (DON), (C) dissolved inorganic nitrogen (DIN), (D) nitrate + nitrite (NO_x) and (E) NH_4^+ in surface and bottom waters at the 9 stations analyzed. Closed circles are surface samples and open circles are bottom samples. X-axis is distance from east to west, starting from station A4. Errors bars represent the 95% CI. If the CI crosses zero, the rate is considered not significant.

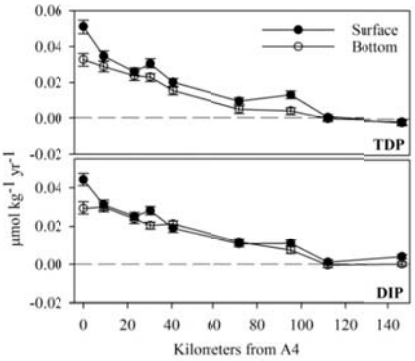

Figure 1.3: Rates of change in concentrations of (A) total dissolved phosphorus (TDP) and (B) dissolved inorganic phosphorus (DIP) in surface and bottom waters at the 9 stations analyzed. Closed circles are surface samples and open circles are bottom samples. X-axis is distance from east to west, starting from station A4. Errors bars represent the 95% CI. If the CI crosses zero, the rate is considered not significant.

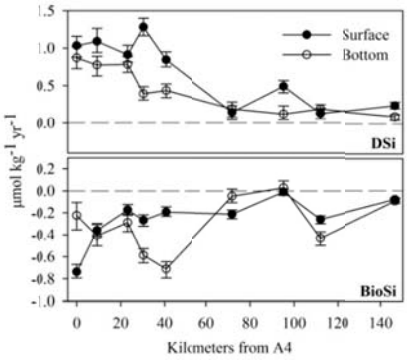

Figure 1.4: Rates of change in concentrations of (A) dissolved silica (DSi) and (B) biogenic silica (BioSi) in surface and bottom waters at the 9 stations analyzed. Closed circles are surface samples and open circles are bottom samples. X-axis is distance from east to west, starting from station A4. Errors bars represent the 95% CI. If the CI crosses zero, the rate is considered not significant.

DINxs index significantly decreased at all stations in surface and bottom waters (Fig. 1.5A). The largest changes were observed in western LIS. Negative trends in DINxs indicated increasing nitrogen-limitation of the phytoplankton community. The DIN:DSi ratios remain unchanged for all stations.

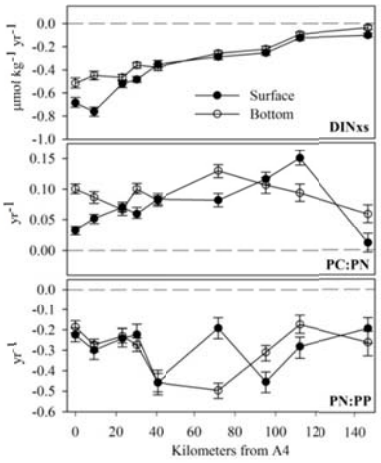

Figure 1.5: Rates of change in (A) the DINxs parameter, (B) the PC:PN ratio, and (C) the PN:PP ratio in surface and bottom waters at the 9 stations analyzed. Closed circles are surface samples and open circles are bottom samples. X-axis is distance from east to west, starting from station A4. Errors bars represent the 95% CI. If the CI crosses zero, the rate is considered not significant.

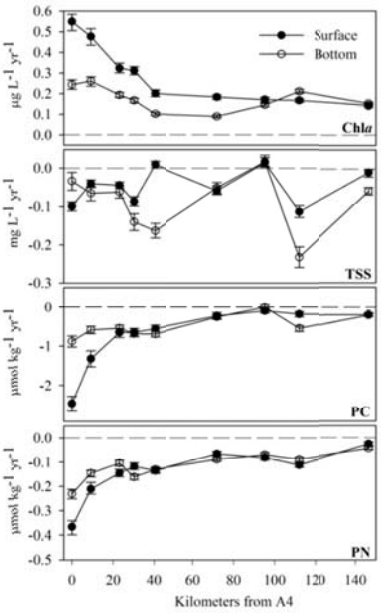

Figure 1.6: Rates of change in concentrations of (A) Chl*a*, (B) total suspended solids (TSS), (C) particulate carbon (PC), and (D) particulate nitrogen (PN) in surface and bottom waters at the 9 stations analyzed. Closed circles are surface samples and open circles are bottom samples. X-axis is distance from east to west, starting from station A4. Errors bars represent the 95% CI. If the CI crosses zero, the rate is considered not significant.

Chl*a* significantly increased at all 9 stations in surface and bottom water (Fig. 1.6A), whereas TSS shows a significant decrease everywhere. Furthermore, particulate carbon and nitrogen (PC, PN) concentrations, which include both living and detrital carbon or nitrogen, significantly decreased at all stations in surface and bottom waters, particularly in the west (Fig. 1.6C-D). There were no measurable changes in particulate phosphorus (PP). Therefore, phytoplankton biomass has increased and detrital and non-photosynthetic planktonic biomass have decreased.

The ratio of particulate carbon: nitrogen concentrations (PC:PN) significantly at most stations in surface and bottom water (Fig. 6B). While the stocks of PC and PN have both decreased, this change in ratio was due to more dramatic declines in PN concentrations than for those of PC. The ratio of particulate nitrogen to phosphorus concentrations (PN:PP) has significantly decreased at all stations in surface and bottom water. Combined changes in the PC:PN, PN:PP, and PN:BioSi ratios strongly suggest that the planktonic community has become increasingly depleted in N and Si relative to C or P.

There were no significant long-term trends in salinity or density. However, there were small but significant decreases in surface and bottom water temperatures, River discharge, precipitation, wind energy, and DO concentrations. Cloud cover exhibited slight but significant decreases.

Objective 2: Examine the role of phytoplankton biomass, bacterial production and mortality on the oxygen demand in the water column.

Chlorophyll a:
Chl*a* was measured from samples collected from 1 meter below the surface at station 1 and integrated through the mixed layer. Integrated Chl*a* inventories were slightly higher in surface waters in September than in August. The majority of Chl*a* was found in the <5-µm fraction. Chl*a* measurements were also taken at depth during each cruise. During the August cruise, the <5-µm size fraction contributed the largest portion of Chl*a* at all depths. During the September cruise, the <5-µm fraction made up the largest portion of Chl*a* in the surface but the contribution of the <5-µm fraction decreased with depth. Chl*a* concentrations in mid-August 2010 were similar to those measured in 2009 (~ 30 µg/l). However, concentrations in mid-September 2010 were higher (~30 µg/l) than they were in September 2009 (~10 µg/l).

Integrated Primary Production:
Surface samples (1 m depth) were collected at station 1 and incubated under graded levels of irradiance (I = 2.5 37.5, and 56.7% I_0) for 24 hours. Rates of primary production were measured by ^{14}C-bicarbonate incorporation and then integrated through the photic zone. Results showed that rates of primary production in August and September of 2010 were less (0.5-2.0 $gC/m^2/d$) than rates during the same time period in 2009 (1.0-4.0 $gC/m^2/d$). Similar to August 2009, net primary production in the August 2010 <20-µm fraction was enhanced compared to unfractionated samples, suggesting that primary producers were culled significantly by larger grazers during that period.

Bacterial Net Production
Bacterial net production (BNP) was estimated from the incorporation rate of ^{3}H-leucine into protein during 3-hour dark incubations. BNP was greatest at mid-depth in August while it was highest in surface and bottom waters in September. Water column integrated BNP in August 2010 was the highest recorded during this 2-year study (~100 $mgC/m^2/d$). Water column integrated BNP in September 2010 (~10 $mgC/m^2/d$) was less than rates measured during mid-September in 2009 (27 $mgC/m^2/d$).

Nutrient analysis
Particulate organic carbon (POC) and particulate organic nitrogen (PON) concentrations were similar in August and September 2009. Overall, the average POC:PON ratio for station 1 throughout this study was 9.9. This exceeded the Redfield ratio for carbon: nitrogen (6.625), suggesting that plankton communities in western Long Island Sound are enriched in carbon relative to nitrogen. The average concentration of ammonia (NH_4^+) was significantly lower in August and September of 2010 (0.6 µmol/kg) than in 2009 (3.3 µmol/kg), and was below detection in several samples. Concentrations of NO_3^-, NO_2^-, and PO_4^{3-} are pending analysis by the SoMAS Analytical Laboratory.

Potential Respiration Rates
Rates of respiration in bottom water in August and September of 2010 were much less than in 2009. Respiration in surface water was always higher than in bottom water. High rates of bottom water respiration in August and September of 2009 (up to 195 µM O_2/d in August 2009) coincided with events of bottom water hypoxia and anoxia. However, in August 2010, we observed bottom water hypoxia at station 1 when respiration rates were only ~ 40 µM O_2/d. In September 2010, bottom water hypoxia was not observed and respiration rates were low (~ 7 µM O_2/d).

Respiration in the <20-µm fraction comprised the largest fraction of total respiration, making up an average 78% of the total respiration observed. Respiration in the <5-µm fraction was usually greater than the respiration in the whole fraction. This was also evident in samples from 2009. This enhancement may be due to decreased grazing pressure on the microbial community after the removal of predators, or due to release of intracellular organic matter derived from filtration-caused cell lysis. We are currently trying to determine which of these explanations is most probable based on results from the other experiments.

Statistics

A statistical analysis of all of our data revealed some significant correlations between biological variables. For example, BNP and dissolved oxygen concentrations are significantly negatively correlated ($r = -0.70$, $p = 0.01$), bacterial abundances and respiration rates in the <20-µm fraction are significantly correlated ($r = 0.71$, $p=0.01$), bacterial abundances and concentrations of POC and PON are significantly correlated ($r = 0.75$, $p = 0.004$ and $r = 0.75$, $p = 0.005$ respectively), bacterial abundances and Chl*a* are significantly correlated ($r = 0.86$, $p = 0.04$), BNP in the <20-µm fraction and POC:PON ratios are significantly correlated ($r = 0.92$, $p = 0.03$), chemoautotrophy and respiration in the <20-µm fractions are significantly correlated ($r = 0.64$, $p = 0.04$), chlorophyll a is significantly correlated with POC ($r = 0.97$, $p = 0.001$) and PON ($r = 0.89$, $p = 0.03$), and chlorophyll a is significantly negatively correlated with total dissolved inorganic nitrogen ($r = -0.93$, $p = 0.005$) and POC:PON ratios ($r = -0.95$, $p = 0.005$).

Objective 3: Develop a 1-D biogeochemical model to determine the mechanistic links between oxygen, phytoplankton biomass, microbial respiration, protistan grazing, stratification, and vertical and horizontal mixing.

General Ocean Turbulent Model (GOTM)

The physical model applied in this study is the Public Domain water column model GOTM (General Ocean Turbulence Model, see http://www.gotm.net) originally published by Burchard et al. (1999) and developed since then (see Umlauf et al., 2005, Burchard et al. 2005). GOTM is a one-dimensional water column model for hydro-thermodynamical processes with vertical mixing. The core of the model solves the one-dimensional transport equations of heat, momentum and salt with mean and turbulent fluxes. The momentum and turbulent equations for GOTM are described in great details in Umlauf et al., 2005 and Burchard et al., 2005. For brevity, these equations are skipped.

Biogeochemical model (Neumann et al. (2002) ERGOM ecosystem model)

The biogeochemical model, viz., Neumann et al. (2002) ERGOM ecosystem model simulates 10 state variables. Among the 10 state variables, ammonium, nitrate and phosphate represent three nutrient state variables. There are three phytoplankton groups and they are Diatoms, Flagellates and Cyanobacteria, respectively. Diatoms represent large-cell phytoplankton and they favor nutrient-rich turbulent environment. Flagellates are smaller-cell phytoplankton, which tend to grow faster in stable water column with lower nutrient concentration. Cyanobacteria are the atmospheric nitrogen fixer and thus provide a nitrogen source for the ecosystem. Three groups of phytoplankton can be grazed by zooplankton dynamically. Dead particles of phytoplankton and zooplankton are accumulated in detritus, which is labile in ERGOM and could be remineralized into dissolved ammonium and phosphate as they are sinking. Some of the detritus could reach the bottom and get accumulated in sediment detritus. Beside surface flux, the dynamics of dissolved oxygen (DO) is coupled to the associated biogeochemical processes (i.e. photosynthesis, respiration, exudation, remineralization and nitrogen fixation) via stoichiometric ratios. DO concentration controls biochemical processes such as denitrification and nitrification in turn.

1-D coupled model

There is a two-way coupling between GOTM and ERGOM. The biogeochemistry of ERGOM depends on the physics provided by GOTM. For instance, all the biogeochemical variables need to go through the vertical mixing to complete their dynamic cycle; temperature is an important control factor on most of the biogeochemical processes such as uptake, grazing, nitrification and nitrogen fixation; phytoplankton photosynthesis and nitrogen fixation are functions of light availability. The water column physics of GOTM was modified by the feedback loop provided by the biogeochemistry of ERGOM. Water column viscosity and density may be changed by the biogeochemical properties. This two-way coupled 1-D physical-biogeochemical model GOTM/ERGOM was applied to study the seasonal variability of oxygen dynamics of Station A4 in western Long Island Sound (LIS) (see Fig. 3.1 for the model structure)..

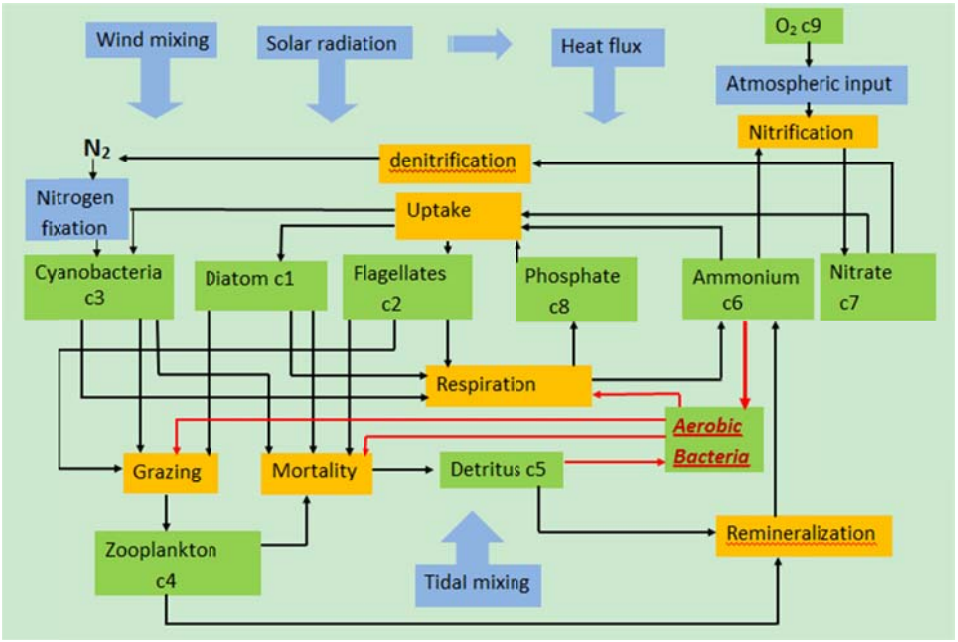

Fig. 3.1: Basic structure of 1-D GOTM/ERGOM. The ten variables are in green boxes; physical forcing is denoted by blue boxes; orange boxes contain all biogeochemical processes; added bacteria box and its associated processes are indicated in red. Note: There is in fact very little cyanobacteria fixing N2 in LIS. The seasonal variability of observed cyanobacteria is assimilated into our model.

Enhancement of coupled 1-D model and results

In order to achieve the goal of determining the mechanistic links between oxygen, phytoplankton biomass, microbial respiration, zooplankton grazing, stratification, and vertical mixing, the current 1-D coupled model should be enhanced to include the bacterial activities and associated oxygen production/demand processes. Before doing this, some of the existing model processes were modified to allow the seasonal variability of the existing state variables and their interrelationships to evolve properly.

To simulate the seasonal variability of water column structure precisely, we decided to nudge the temperature and salinity within top 5 m of the water column with the observations in GOTM. By doing so, not only the seasonal evolution of physical properties was well developed, the vertical structure of water column properties was also allowed to be simulated by GOTM.

The model skill of GOTM was analyzed to find out the suitable nudging time scale and minimum mixing scheme k_z. We developed an enhanced symmetric model skill metric $S4 = 1.0 - (e^{-\frac{(\sigma_x - 1.0)^2}{0.18}})(e^{-\frac{(R-1.0)^2}{0.18}})$ in order to equally assess the standard deviation and correlation coefficient. The old model skill metric (i.e. $S3 = 1.0 - (e^{-\frac{(\sigma_x - 1.0)^2}{0.18}})(\frac{1+R}{2})$) applied in Joliff et al., 2009 was asymmetric and could result in unequally weighted statistical properties, so the target parameters may not be properly chosen. By minimizing the enhanced model skill metric S4, we applied the best minimum mixing scheme $k_{\min} = 2 * 10^{-5}$ and an optimum nudging time scale one month for both temperature and salinity in GOTM. To allow the model to adjust to proper initial conditions, it was spin up for 7 years and only the last year's results are analyzed.

In ERGOM, three nutrients species (i.e. ammonium, nitrate and phosphate) and phytoplankton groups (i.e. diatom, dinoflagellates, cyanobacteria) were nudged with three-month relaxation time scale toward monthly averaged observations from 2002 to 2010. The purpose was to ensure the seasonal evolution of major nutrient and phytoplankton species properly developed so that the role of bacterial activity in determining seasonal variability of DO could be established on top of accurate mechanical linkages of the ecosystem.

Bacterial biomass was added into ERGOM as an additional box (see Fig. 3.1) and bacterial activities including bacterial respiration were added into the model. Besides substrate control, a temperature control factor was added into the bacterial respiration and uptake activities. Labile detritus remineralization was substituted by two major processes, i.e., bacteria uptake of detritus process and bacterial exudation into inorganic nitrogen. In the enhanced model, labile detritus composed of Dissolved Organic Nitrogen (DON) was assumed to be the major carbon source of bacteria. Bacteria also assimilate ammonium to obtain nitrogen. In steady state, the amount of ammonium uptake by bacteria depends on the C:N ratio of dissolved organic matter (DOM), bacterial biomass, and the growth efficiency of bacteria for carbon and nitrogen. In addition, bacteria are consumed by zooplankton, which is represented in our model as a function of seasonal cycle of temperature, concentration of the prey and predators. The feedback loop of bacterial activity to the planktonic loop was mainly composed of bacterial exudation and mortality in the enhanced model. Bacterial mortality contributes to increase of labile DON; bacteria exudation led to increase of inorganic nitrogen.

The challenging part of this objective was how to include the bacterial activity loop in the model. Because oxygen is consumed when labile detritus eaten by bacteria, the bacterial oxygen consumption process in the model was linked to detritus uptake by Stoichiometric O:N ratio.

Objective 4: Elucidate relationships between late summer oxygen recovery, phytoplankton biomass, bacterial production/mortality, vertical mixing, and horizontal advection.

To achieve this objective, we first examined the physical and biogeochemical properties. In addition, we proposed a mechanism of late summer oxygen recovery related to vertical mixing and bacterial activities (i.e., bacterial respiration, production, mortality, etc).

Water column properties

Our model result of the seasonal cycle of sea surface temperature (SST) (see Fig. 4.1a) has the minimum value 2.5^{o}C in middle February. In April the surface water warms up to between 6 and 10^{o}C, and it maximizes at 22 ^{o}C in early September. Starting from middle February, SST increases gradually until early September, after that it linearly decreases toward early December. The bottom waters in early September reach the maximum temperature 22^{o}C. The vertical structure of temperature (Fig. 4.1b) is well mixed between January and April. Starting from May the thermocline starts to develop approximately 15m below the surface, and then it shoals gradually with time. The thermocline becomes shallowest (i.e., 4m) in July. After that it starts to deepen and the water column becomes well mixed again from September to December. Modeled temperature (Fig. 4.1b) in

general has similar seasonal variability and magnitude as the observations. The model underestimates a little of the MLD in May and June. However, according to results of model skill analysis, our choice of k_{min} and nudging time scale gets the best fit.

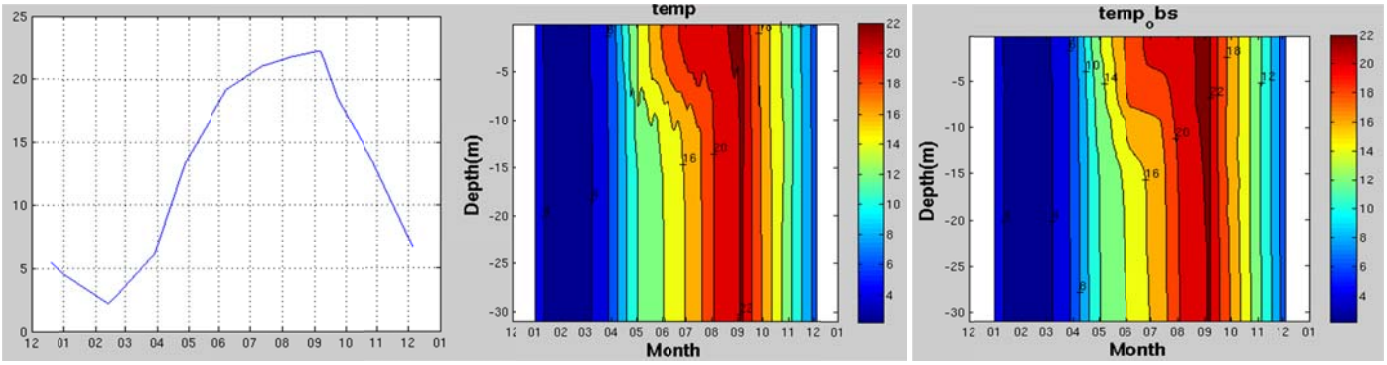

(a) (b) (c)

Figure 4.1 (a) Sea Surface Temperature. (b) Seasonal variability of modeled temperature profiles. (c) Seasonal variability of observed temperature profiles.

The Sea Surface Salinity (SSS) (Fig. 4.2a) decreases almost linearly from the maximum level in early January to the minimum level at the end of April. Then it increases linearly to 26.25 g/kg toward early July. After that there is a small decrease to 26.15 g/kg by early August and then it increases linearly to reach a secondary maximum level 26.5 g/kg at the end of September. Thereafter, the salinity falls below 26 g/kg by the end of the year. Vertical structure of salinity (Fig. 4.2c) differs from temperature in several aspects. Vertical salinity gradients in LIS were relatively weak during the summer season compared to temperature with the maximum difference 1 g/kg between the surface and bottom in February, while temperature differences could reach almost 8^{o}C. It is stratified almost the whole year. Salinity falls below 25.5 g/kg from middle March to late June throughout the whole water column and reaches minimum value in April at the surface. As summer turns to fall, the vertical gradients in salinity remain relatively strong with the surface and bottom salinity difference 0.5 g/kg. The simulated salinity (Fig. 4.2b) generally agrees with the observation in terms of its seasonal variability and magnitude, except that in February and March the modeled vertical salinity structure tends to have deeper halocline.

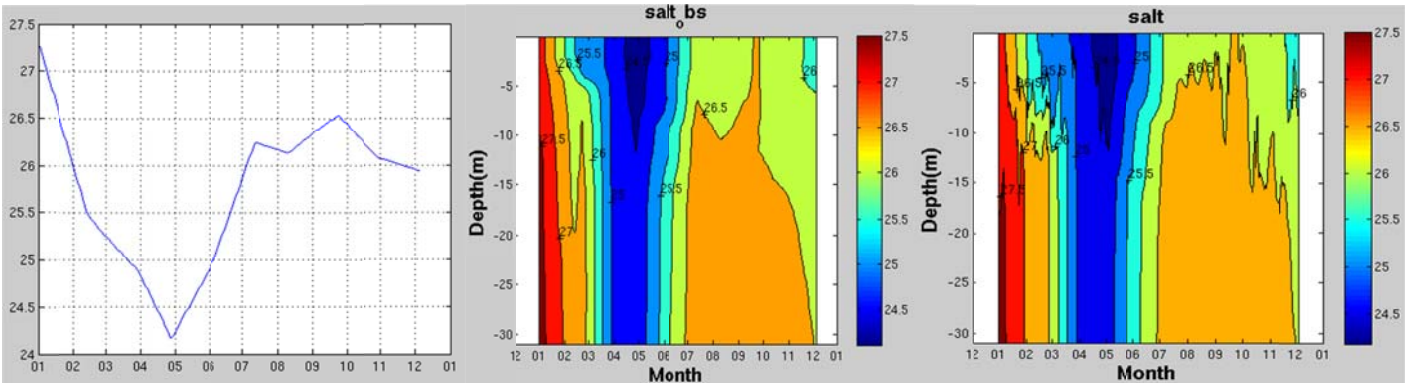

(a) (b) (c)

Figure 4.2 (a)Sea Surface Salinity. (b) Seasonal variability of modeled salinity profiles. (c) Seasonal variability of observed salinity profiles.

Seasonal variability of biogeochemical properties

According to our result, the bottom ammonium (Fig. 4.3a) reaches its maximum of 11 mmol N m^{-3} in January, and then starts to decrease until end of May, after which there is a gradual increase towards December. For most of the time, the simulated bottom ammonium agrees well with the observations. Nitrate concentration shows much less seasonal variability than ammonium. The bottom nitrate (Fig. 4.3b) has the maximum concentration 5 mmol N m^{-3} in January. Then it decreases to 0.3 mmol N m^{-3} in May, and remains more or less constant until November. In December it increases to 3.5 mmol N m^{-3}. Phosphate concentration at bottom (Fig. 4.3c) exhibits similar seasonal cycle as ammonium although differing in the variability. Similar to ammonium and nitrate, in the beginning of the year, bottom phosphate has maximum concentration 1.2 mmol N m-3. Then it decreases almost linearly to minimum 0.2 mmol N m^{-3} at the end of June. After then it increases step like to 0.9 mmol N m^{-3} by the end of the year. Simulated bottom phosphate behaves very similar as the observation although showing higher increasing rate in September and October.

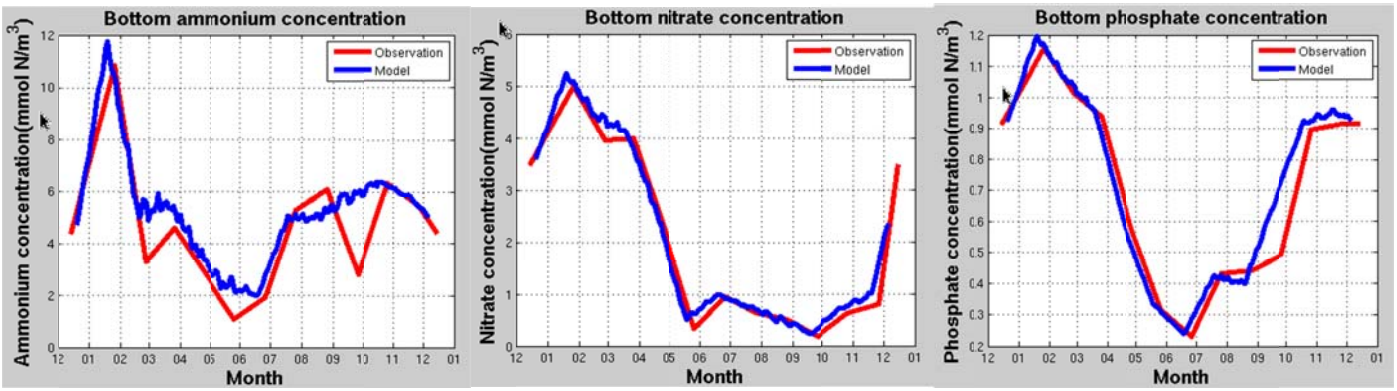

(a) (b) (c)

Fig. 4.3a: Modeled bottom ammonium time series compared with observations. Fig. 4.3b: Modeled bottom nitrate time series. Fig. 4.3c: Modeled bottom phosphate time series.

The simulated Stoichiometry Ratio of N/P shown in Figure 4.4 tends to peak twice with peaking value around 14 in January and August, which are about the time when bloom occurs. In addition, the fact that Stoichiometry Ratio is consistently below 16 (see results for objective 1 above) suggests that phosphate was available in excess of biological requirements rather than demonstrating nitrogen limitation in LIS supporting previous investigations (e.g., Anderson & Taylor,2001).

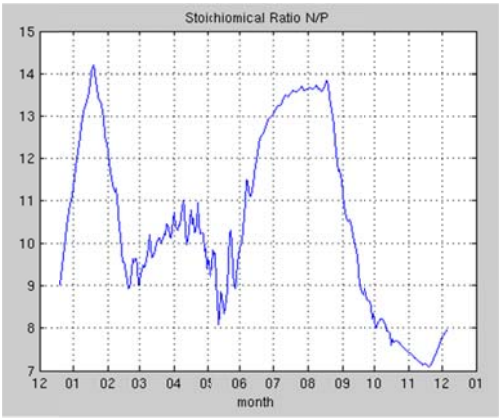

Figure 4.4: Seasonal variation of Stoichiometry Ratio N/P. N represents sum of ammonium and nitrate concentration; P indicates phosphate concentration.

Seasonal variation of oxygen concentration is also controlled by biological activity. Modeled surface diatom concentration versus observation is plotted in Figure 4.5a. Surface diatom shows two peaks with concentration of 4.5-5 mmol N/m^3 at mid-April and mid-July, representing the spring and summer diatom blooms. In the

beginning of the year, diatom concentration is as low as 0.5 mmol N m^{-3}. Then it increases quickly to 4 mmol N m^{-3}, and this is a secondary diatom peak before the first diatom bloom. After that the concentration goes up to 4.75 mmol N m^{-3} in April. Between the two peaks, diatom concentration exhibits a minimum concentration of 2.3 mmol N m^{-3}. Our result of spring bloom is consistent with previous findings of phytoplankton bloom in LIS, which indicate that winter spring bloom could begin as early as January, mostly in February, but could also be delayed until March or later (Capriulo et al., 2002; Riley, 1969). The summer diatom bloom occurs in July and the relatively high diatom biomass sustains throughout the summer seasons. It is possibly triggered by interruption of fall destabilization due to combination of increased temperature and river discharge, as well as reduced winds (Riley, 1959; Capriulo 2002). After that, diatom biomass decreases toward the end of year to the original level. In general, the phase of simulated diatom variability is approximately 10 days later than the measurements before middle September, after which the model tends to agree well with the measurements.

Seasonal variation of dinoflagellate biomass exhibits less variability and smaller amplitude compared to diatom. At surface the biomass (Fig. 4.5b) starts to increase gradually from 0.1 mmol N m^{-3} in January to 0.2 mmol N m^{-3} in late April, after that it increases sharply till reaching 0.6 mmol N/m^3 in middle June, which stays almost constant from mid-June till mid-September, when diatom has already died out. Previous studies indicate that flagellates bloom in LIS may happen in June with sufficient nitrogen supply (Riley & Conover, 1967), and may replace the diatom biomass as the season progresses because flagellates are favored by stratification and low inorganic nitrogen more than diatoms (Capriulo 2002; Riley & Conover, 1967; Demers et al., 1978; Margalef, 1978; Mann, 1982; Peterson, 1986; Mann & Lazier, 1991; Kiørboe, 1993). After the bloom, the Dinoflagellates biomass decreases sharply toward the end of the year. The simulated dinoflagellates biomass exhibits similar seasonal variability and magnitude as the observation.

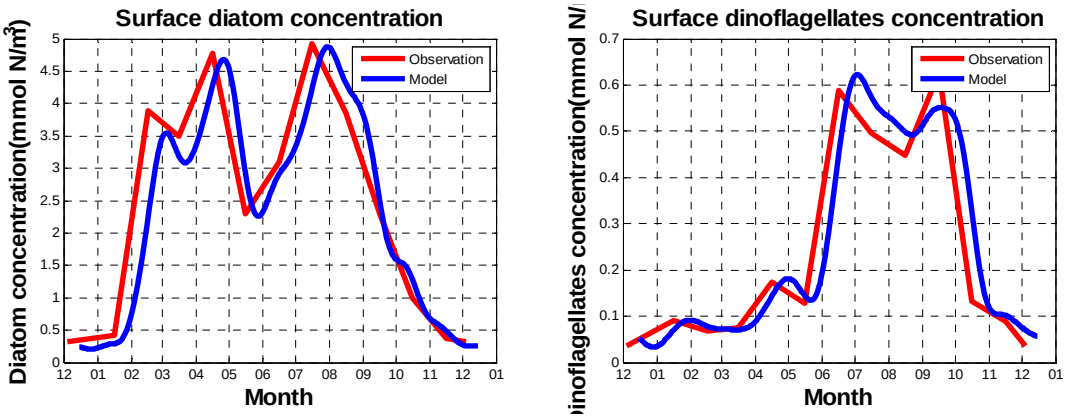

(a) (b)

Figure 4.5: Seasonal variation of diatom and dinoflagellates. Fig. 4.5a and Fig. 4.5b show profiles of diatom and dinoflagellates, respectively. Blue line shows model results, which is nudged with five-day relaxation time scale using monthly climatological data, indicated by red line.

The simulated bacterial concentration as a function of depth and time is shown (Fig. 4.6a). For comparison purpose, the time series of observed bacterial concentration measured at surface versus the modeled concentration is plotted (Fig. 4.6b). The modeled bacterial biomass at surface shows the same order of magnitude as the observed surface bacteria concentration (Fig. 4.6b). The initial concentration is 0.2 mmol N m^{-3}, then it starts to increase to 1 mmol N m^{-3} and sustains at that level through May. After that it increases quickly to the maximum 3 mmol N m^{-3} in July and August. Thereafter the biomass just goes down to the original low level by the end of the year. The seasonal variation of bacterial biomass profile (Fig. 4.6a) shows that the surface bacteria concentration reaches maximum of 3mmol N m^{-3} at the top 5 m during summer, below which it decreases with depth to approximately 1mmol N m^{-3}.

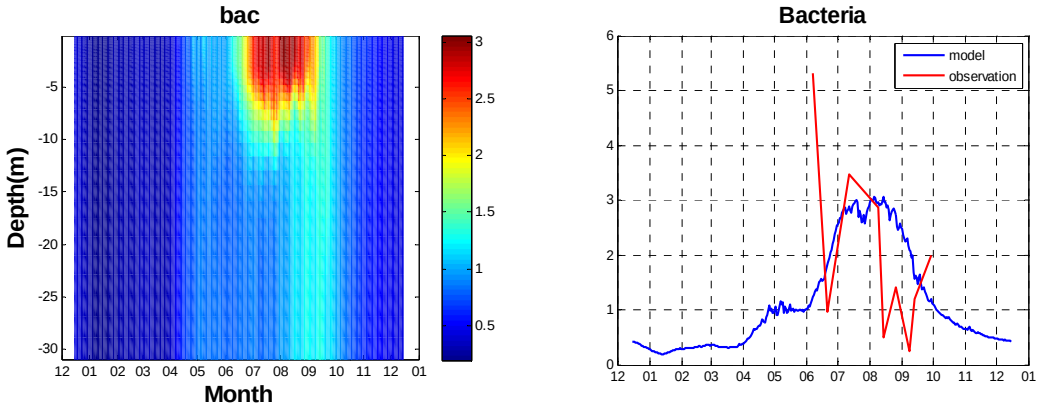

(a) (b)

Figure 4.6a: Seasonal variation of bacterial profile. Figure 4.6b: seasonal evolution of bacterial biomass at the surface. Red line indicates observed bacterial concentration of June, July, August and September. Blue line represents simulated model result for the whole year.

With the complete bacterial loop, the annual cycle of simulated bottom oxygen generally agrees well with the observations (Fig. 4.7b). The measured bottom oxygen maintains at high level (i.e. 10.5~11.5 mg O_2/L) from January to April. After that both the model and observation show linear reduction of bottom DO with fast decreasing rate (i.e. approximately 3 mg O_2/L per month) to the minimum level (i.e. 0.3~0.5 mg O_2/L) in middle August. Then the bottom DO starts to recover from hypoxia. The model successfully captures a small decrease of bottom DO in early September during the general increasing progress. It seems that after this point, the model overestimates the increasing rate of oxygen relatively to the measurement. The oxygen profile as a function of time within one year is shown in Figure 4.7a. DO concentration is high (approximately 12 mg O_2/L) from January to May throughout the entire water column, and then the vertical DO structure starts to stratify with the oxygen level below 5 m quickly falling below hypoxic level. Oxygen level oscillates in and out of hypoxia within the water column between 5 and 10 m in depth. Below 10 m hypoxia occurs throughout the whole summer until early September, after which the whole water column recovers from hypoxia with much less vertical oxygen gradient. The precise representation of seasonal variability of oxygen by our enhanced model proves that adding bacterial loop and its associated oxygen consumption process is a critical step in model simulation. This also suggests that with the added bacterial remineralization of DON and its associated oxygen consumption process, seasonal development of oxygen could be accurately simulated without necessity of distorting vertical mixing or phytoplankton.

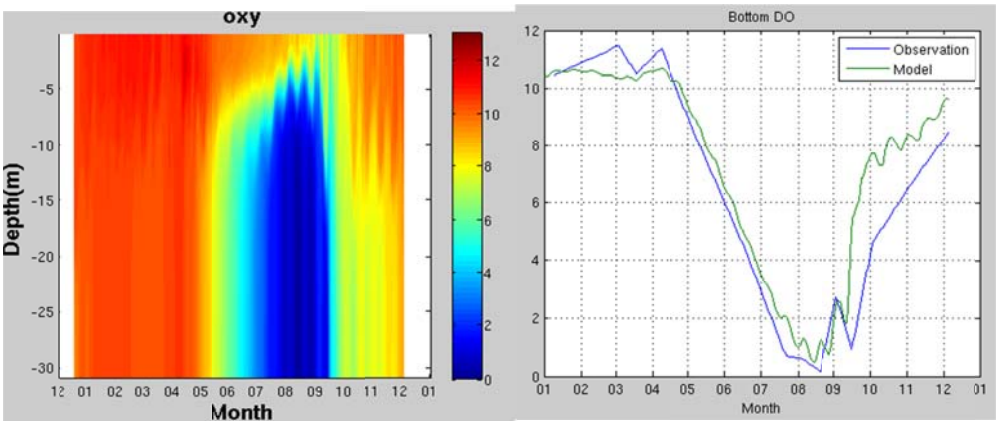

(a) (b)

Figure 4.7: Seasonal variation of DO. (a)Simulated variability of DO profile. Figure (b) Simulated seasonal variation of bottom DO in comparison with the observation.

The importance of bacterial loop in simulating seasonal hypoxia

Examining the role of bacterial activity in regulating seasonal variability of DO is important, because the recovery of DO from minimum levels in late summer or early fall has generally been accepted to be a result of increased wind mixing from summer low (O'Donnell et al., 2008). If this is the case, the timing of DO recovery should be sensitive to change of increase in wind mixing. However, Lee & Lwiza (2008) showed that the recovery of hypoxia is not necessarily driven by increased mixing. In order to test this point, we postponed the input wind forcing by one month so that the increase of wind forcing is postponed to the same extent in the model. The results are compared with the previous model results without postponing the wind. As seen in Figure 4.8, neither the phase nor amplitude of bottom DO has changed as the increase in wind stress is postponed by one month. The hypoxic condition still occurs in late August, and the timing of recovery of hypoxia is not postponed in response to the postponement of wind mixing. Therefore, from our model results we concluded that the relaxation of hypoxia is not sensitive to increase of wind mixing alone. 1

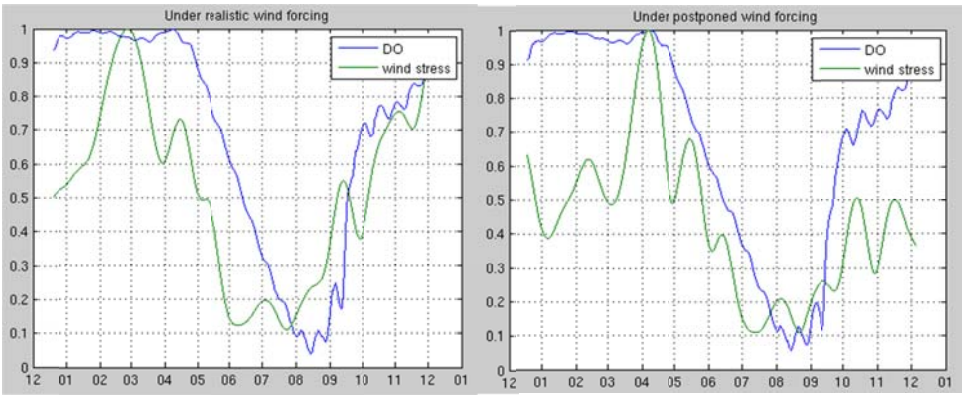

(a) (b)

Figure 4.8: Relationship between bottom DO and surface wind stress. Figure 4.8a: Model results under realistic wind forcing. Figure 4.8b: Model results under wind forcing postponed by one month.

In order to examine how the variability of bottom DO will be influenced by the bacterial activities, we remove the whole bacterial loop and associated oxygen consumption processes in the model. Without any further model tuning, the resulting seasonal DO profile under realistic mixing condition is shown in Figure 4.9. Before May the DO concentration (i.e. approximately 11-12 mmol O_2 m^{-3}) is close to the one before removing bacterial loop. Starting from July, the decreasing trend of bottom DO in the case without bacteria stops at about 7 mmol O_2 m^{-3}, whereas in the model with bacterial loop the decrease trend of bottom DO lasts until early September and reaches as low as 1 mmol O_2 m^{-3} in late August and early September. After October, bottom DO with and without bacterial loop both increase and converge to about 11 mmol O_2 m^{-3}. The result that without bacterial loop the summer bottom oxygen is much higher than the one with bacterial loop implies that without bacterial loop, just changing the vertical mixing alone cannot obtain a reasonable representation of hypoxia (O'Donnell et al. 2010, Hydroqual 2003), even though many previous model studies suggested that the variability of the near bottom oxygen levels is mainly affected by the vertical mixing (O'Donnell et al, 2008, McCardell and O'Donnell, 2009).

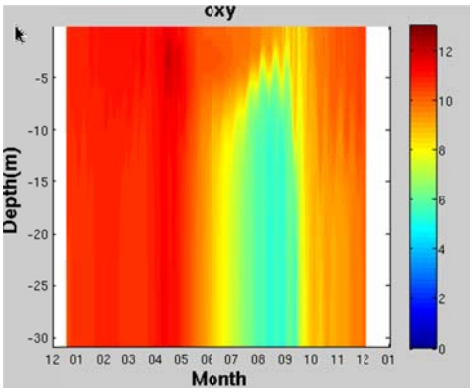

Figure 4.9: Simulated seasonal variability of DO without bacterial activity.

Therefore, our findings strongly support the proposition that the major mechanism controlling seasonal oxygen variability is bacterial activity since bacterial biomass depends on organic carbon availability, and its feedback loop to the entire planktonic loop modulates organic carbon remineralization, hence the link to oxygen variability. Phytodetritus (i.e., detritus) is the major source of labile carbon, which comes from mortality of phytoplankton and zooplankton, settles down into sediment fluffy layer, and is remineralized into inorganic matter by bacteria (Anderson & Taylor 2001). Detritus thus occupies the key position in the entire ecosystem and connects the bacterial loop to all the other biogeochemical components. In addition to controlling oxygen dynamics, remineralization of detritus is important to the entire biogeochemical cycle because it converts primary production into bacterial production, enabling inorganic nutrients to be returned to the water column and further feed primary production via the feedback loop (Anderson & Taylor 2001; Welsh & Eller 1991).

C2. Scientific Abstract:

Between 1995 and 2009 all stations in the western and central basins of LIS exhibited significant changes in nutrient dynamics. Inorganic phosphorus concentrations increased across the whole Sound, while bottom water temperatures show a slight decrease at several stations. These results suggest that phytoplankton has shifted to a community that is more dependent on organic sources of nutrients, making organic phosphorus a more important source of P. This would decrease the assimilation rate of DIP and cause it to accumulate in the water column. However, there is an alternative process that could explain the DIP increase, i.e., increased PO_4^{3-} loadings brought in by wastewater. The main source of PO_4^{3-} into western LIS is sewage contamination from the East River. Since 1992, New York City started adding ortho-phosphoric acid to all drinking water supplies (Maas et al., 2005), may have increased the concentration in the wastewater. Another interesting result is that since DSi concentrations increased Diatom abundances were expected to increase. However, diatom abundances declined in the western and central basins, whereas silica concentrations increased. This characteristic of diatom decrease (indicated by BioSi concentrations) as the degree of eutrophication decreased while the PN:BioSi ratios remained unchanged indicates that DIN, instead of DSi, was the limiting macronutrient for diatoms. In general, DIN species at most stations declined in favor of DON while total nitrogen has decreased. We think the declines in DIN driven by decreased anthropogenic loadings. There is also a strong evidence of a regime shift in planktonic biomass in LIS. The changes in biomass composition are likely due to increased DIN-limitation. Statistical analysis of the field data obtained by this project suggest that the majority of the organic carbon in western Long Island Sound is autochthonous, originating from *in situ* production by phytoplankton. There are strong relationships between the amount of organic matter, bacterial activity, and rates of respiration. Furthermore, an additional source of respiration may be chemoautotrophy by the microbial community.

Results from the coupled model show that the onset of relaxation of late summer hypoxia is not sensitive to increase of wind mixing alone. Seasonal variability of dissolved oxygen is mainly controlled by bacterial activity. This mechanism can be explained as follows: bacterial biomass depends on organic carbon availability,

which in turn ~~depends on planktonic loop~~ modulates organic carbon remineralization, hence the link to oxygen variability. Bacterial processes, including bacterial production, respiration and mortality are very important in modulating organic matter decomposition and oxygen variability in coastal estuaries. Therefore, in order to accurately represent oxygen dynamics coastal ecosystem models should explicitly simulate the whole microbial loop when modeling and predicting oxygen variability. More importantly, this effort revealed major drawbacks which would hamper improvements of models, *viz.*, lack of field measurements of several important rates, e.g. growth and mortality of important groups. There should be concerted efforts to obtain relevant values of these rates. Substantial modifications are required in these models before they can be used by decision makers to reassess and develop more realistic total maximum daily loads (TMDLs) in order to manage hypoxia.

C3. Problems Encountered: (1) We had trouble getting R/v Paumanok, the boat we initially intended to use, because of logistical and manpower issues, but eventually SoMAS provided us with a bigger boat R/v Seawolf at the price of the smaller boat. (2) We could not obtain data on sediment oxygen demand from Principal Investigators working on a sister LISS-funded project during the same funding cycle. (3) We did not have measurements for growth, mortality rates for bacteria, phytoplankton and zooplankton major groups, as well as grazing and exudation rates for zooplankton from LIS.

C4. New Research Directions: Identify additional, new research directions pursued during the course of the project, and reasons for adding them to the original research plan. Also, list any newly funded projects resulting from this NYSG project.

1. Invest in field programs that would determine fundamental ecological rates, for example:

    a. Growth and mortality rates of important phytoplankton species as a function of nutrients, light, temperature, depth and time (season). We are cognizant of the expenses involved, but three or four depths in the water column would suffice.

    b. Grazing growth and mortality rates of important zooplankton species as a function of phytoplankton group biomass (and/or bacteria), depth temperature, and time (season).

    c. Excretion rates of important zooplankton species as a function of phytoplankton biomass, depth and time (season).

    d. Growth and mortality rates of important bacterial groups as functions of temperature, nutrient regimes, depth and time (season).

    e. Nitrification/denitrification rates.

    f. Sediment oxygen demand processes need to be better resolved temporally and spatially.

2. Invest in coupled 1-D models or simple 3-D models (with 3x3 grids) that are easy to analyze in order to make sure that we have most if not all fundamental ecological processes covered properly (not hastily parameterized). Combined with item (1) above this would minimize the model uncertainty in very significant way. Currently, there are models that use 22-30 state variables, with very little knowledge about how those variables interact in the field.

3. Follow the path of climate modelers by using inter-comparison between different models to identify gaps in our understanding how processes involved in oxygen dynamics work. Other regions like the Chesapeake Bay have already started doing this, but in Long Island Sound there is still fear in using this approach. The fear is based on the argument that – "***what happens if we find that SWEM is fundamentally flawed or just performs poorly compared to other models, after having invested large amount money?***". However, this fear is unfounded because competition will force SWEM supporters to improve the code. If for some reason it cannot be improved then superior alternatives should be considered.

C5. Interactions: Describe participation or interactions with NYSG Extension staff, and industry, agency or other stakeholder representatives.

1. In March 2009 we organized a meeting for the newly funded U.S. EPA projects at Stony Brook. We invited the Director of New York Sea Grant, Dr. J. Ammerman. The purpose of the meeting was to explore ways to integrate field work where possible and share data. We wanted to develop a coordinated field effort to maximize the resources.
2. The PI worked with New York Sea Grant to convene a meeting at Stony Brook On April 27, for all newly funded and ongoing projects in LIS funded by U.S. EPA through LISS, New York Sea Grant, and Connecticut Sea Grant. Similar to the earlier internal meeting for Stony Brook investigators, the purpose of the meeting was to examine current knowledge of what was being addressed by the funded projects and examine was of coordinating the field work and encourage data sharing.
3. All project personnel attended all STAC meetings that were held during the lifetime of the project. We presented our results and made suggestions on how to improve observations, models, and their interpretation.
4. We exchanged field data with James O'Donnell of the University of Connecticut. He gave us time series data from the Execution Rocks Buoy.

C6. Presentations and Publications:

Publications:

None (We have two manuscripts ready to be submitted).

Presentations:

1. Kamazima Lwiza, Elizabeth Suter, Gordon Taylor & Ling Liu. March 16th 2010, Long Island Sound Researcher Workshop "Interaction of Biological and Physical Factors Controlling Bottom Dissolved Oxygen"

2. Kamazima Lwiza July 09, 2010, Long Island Sound STAC meeting at the University of New Haven "Spatial and Temporal variability of Nutrients in LIS"

3. Ling Liu and Kamazima Lwiza, The seasonal variability of circulation in Long Island Sound. Middle Atlantic Bight Physical Oceanography and Meteorology. MABPOM 2010. Steve's Institute, New Jersey.

4. Elizabeth Suter & Kamazima Lwiza March 27th 2010, Symposium for SoMAS Student Recruitment Weekend - "Factors Affecting Hypoxia in Long Island Sound"

5. Elizabeth Suter, Gordon T. Taylor, Kamazima Lwiza & Julie Rose May 5th, 2011, Changing nutrient regimes in Long Island Sound: A 15-year analysis. Spring 2011 NEERS Conference (New England Estuarine Research Society), Pt. Jefferson, NY. *BEST POSTER AWARD*

D1. Impacts & Effects:

This project will have profound impacts in resources management the modeling community especially those dealing with hypoxia. Field observations show (i) evidence of measurable success of TMDL because dissolved nitrogen species are decreasing; (ii) an alarming trend of decreasing N:P ratios which is most probably decreasing the diatom biomass in favor of dinoflagellates; (iii) that summer hypoxia continues to occur (with

same magnitude and duration) in bottom waters despite the decreasing trend of dissolved nitrogen species; (iv) phosphorus concentration is increasing in the Sound probably due to addition of phosphorus to drinking water in New York City. Results from modeling experiments underscore the importance of the microbial loop in controlling dissolved oxygen dynamics. Several models being used for both research and operational applications in our coastal areas will have to re-examine their biogeochemical models.

D2. Scholar(s) & Student(s) Status:

1. Elizabeth Suter – Scholar – Completed her MSc in Dec 2011 and she is now doing her PhD under G. Taylor in SoMAS, Stony Brook University.
2. Ling Liu – Scholar – She is still doing her PhD in a her third year under K. Lwiza SoMAS, Stony Brook University.

Other students (not financially supported):

3. Cassandra Bauer (undergraduate): Participated in the first cruise on R/V Pritchard of May 28, 2009. Filtering water samples on board the boat and in the laboratory. Graduated in May 2009 and entered the graduate program in SoMAS, Stony Brook University for MSC and graduated May 2012.
4. Jacob Kalda (undergraduate): Participated in the third cruise on R/V Seawolf of June 23, 2009. Also, has been involved in experiment –setup and field data analysis in the laboratory. Graduated in May 2010.
5. Mariella Lopez-Gasca (MS student): Participated in the first two cruises on R/V Pritchard of May 28, 2009 and on R/V Seawolf of June 23, 2009. Also, has been involved in experiment –setup and field data analysis in the laboratory.
6. Younjoo Lee (Ph.D. Student): Participated in the second cruises on R/V Seawolf of June 23, 2009. He helped in collecting data on water column properties and acoustic Doppler current profiler (ADCP) data. Graduated in May 2009 and is currently a post-doctoral fellow at the University of Maryland.
7. Katie Kennedy (undergraduate): Participated in the October 1st cruise on R/V Seawolf of May 28, 2009, and has been involved in experiment –setup and field data analysis in the laboratory. Graduated in May 2010.
8. Kristin Kramss (undergraduate): Participated in a cruise on R/V Seawolf of October 1st, 2009. Graduated in December 2009.

D3. Volunteers: (None).

D4. Patents: (None).

E. Stakeholder Summary: There is modest evidence that LIS TMDL is working because some nutrients are decreasing, although some continue to increase. Nevertheless, for the last 15 years (1995-2009) summer hypoxia volume and duration in bottom waters have not changed much despite the decreasing trend of dissolved nitrogen species. What is even more alarming is that concentrations of large phytoplankton species (diatoms) which used to be dominant are decreasing in favor of smaller species which could affect the whole food chain in the Sound. There is also evidence to show that the addition of ortho-phosphoric acid to drinking water supplies in New York City in order to protect the population from lead poisoning from old pipes is leading to an increase in phosphorus in the Sound. Results from modeling experiments show that prediction of hypoxia can be improved by including the microbial loop explicitly in dissolved oxygen dynamics.